

1 The Teddy-Tool v1.0: temporal disaggregation of daily climate 2 model data for climate impact analysis

3 Florian Zabel¹, Benjamin Poschlod²
4

5 ¹Ludwig-Maximilians-Universität München (LMU), Department of Geography, Luisenstr. 37, 80333 Munich,
6 Germany

7 ²Research Unit Sustainability and Climate Risks, Center for Earth System Research and Sustainability, Universität
8 Hamburg, Grindelberg 5, 20144 Hamburg, Germany

9 Correspondence to: Florian Zabel (f.zabel@lmu.de)

10 Abstract

11 Climate models provide required input data for global or regional climate impact analysis in temporally
12 aggregated form, often in daily resolution to save space on data servers. Today, many impact models
13 work with daily data, however, sub-daily climate information is getting increasingly important for more
14 and more models from different sectors, such as the agricultural, the water, and the energy sector.
15 Therefore, the open source Teddy-Tool (temporal disaggregation of daily climate model data) has been
16 developed to disaggregate (temporally downscale) daily climate data to sub-daily hourly values. Here,
17 we describe and validate the temporal disaggregation, which is based on the choice of daily climate
18 analogues. In this study, we apply the Teddy-Tool to disaggregate bias-corrected climate model data
19 from the Coupled Model Intercomparison Project Phase 6 (CMIP6). We choose to disaggregate
20 temperature, precipitation, humidity, longwave radiation, shortwave radiation, surface pressure, and
21 wind speed. As a reference, globally available bias-corrected hourly reanalysis WFDE5 data from 1980-
22 2019 are used to take specific local and seasonal features of the empirical diurnal profiles into account.
23 For a given location and day within the climate model data, the Teddy-Tool screens the reference data
24 set to find the most similar meteorological day based on rank statistics. The diurnal profile of the
25 reference data is then applied on the climate model. The physical dependency between variables is
26 preserved, since the diurnal profile of all variables is taken from the same, most similar meteorological
27 day of the historical reanalysis dataset. Mass and energy are strictly preserved by the Teddy-Tool to
28 exactly reproduce the daily values from the climate models.

29 For evaluation, we aggregate the hourly WFDE5 data to daily values and apply the Teddy-Tool for
30 disaggregation. Thereby, we compare the original hourly data with the data disaggregated by Teddy.
31 We perform a sensitivity analysis of different time window sizes used for finding the most similar
32 meteorological day in the past. In addition, we perform a cross-validation and autocorrelation analysis
33 for 30 globally distributed samples around the world, representing different climate zones. The
34 validation shows that Teddy is able to reproduce historical diurnal courses with high correlations >0.9
35 for all variables, except for wind speed (>0.75) and precipitation (>0.5). We discuss limitations of the
36 method regarding the reproduction of precipitation extremes, inter-day connectivity, and
37 disaggregation of end-of-century projections with strong warming. Depending on the use case, sub-
38 daily data provided by the Teddy-Tool could make climate impact assessments more robust and
39 reliable.

40 Introduction

Gelöscht: on a daily basis

Gelöscht: for temperature, precipitation, humidity, longwave radiation, shortwave radiation, surface pressure and wind speed.

[5] nach unten verschoben: Thereby, mass and energy are strictly preserved by the Teddy-Tool to exactly reproduce the daily values from the climate models.

Gelöscht: document

Formatiert: Schriftfarbe: Automatisch

Gelöscht: Therefore

Formatiert: Schriftfarbe: Automatisch

Gelöscht: course

Gelöscht: empirically

Gelöscht: Thereby,

[5] verschoben (Einfügung)

Gelöscht: mMass and energy are strictly preserved by the Teddy-Tool to exactly reproduce the daily values from the climate models.

Gelöscht:

Gelöscht: ,

Gelöscht: and extreme value

Gelöscht: However,

Gelöscht: w

Gelöscht: also

Gelöscht: Consequently

63 Sub-daily climate data is becoming increasingly important in climate impact analysis. This type of data,
64 which captures variations in temperature, precipitation, and other weather variables at intervals of
65 less than a day, can provide a more detailed representation of local and regional climate conditions
66 and temporal variations. This information can be crucial for evaluating the impacts of climate change
67 on various sectors, such as agriculture, water resources, energy production, and human health (Golub
68 et al., 2022; Trinanés and Martínez-Urtaza, 2021; Colón-González et al., 2021; Tittensor et al., 2021;
69 Byers et al., 2018; Jägermeyr et al., 2021; Poschlod and Ludwig, 2021; Degife et al., 2021). A better
70 representation of the diurnal course of temperature, extreme precipitation events, and other weather
71 variables are also important for adaptation assessments which depend on behavior or processes with
72 high temporal dynamics, such as the energy demand, labor activity, the heat stress of crops or flood
73 events (Minoli et al., 2022; Zabel et al., 2021; Reed et al., 2022; Orlov et al., 2021; Franke et al., 2022;
74 [Poschlod 2022](#)). Research has shown that using sub-daily climate data can result in more robust and
75 reliable impact assessments compared to using daily data (Orlov et al. 2023).

76 Today, most climate model data are available for download at daily resolution because of the high
77 storage requirements for sub-daily climate data. However, the demand for sub-daily data is increasing
78 due to lower costs for storage and computing resources. Different methods exist to disaggregate
79 available daily climate data to sub-daily, most often hourly values. These can be roughly divided into
80 statistical methods, weather generators, and mechanistic approaches, although mixed forms also exist
81 (Förster et al., 2016).

82 Mechanistic methods use regional climate models to dynamically downscale atmospheric conditions
83 in time and space, usually for a limited area (Vormoor and Skaugen, 2013; Liu et al., 2011; Kunstmann
84 and Stadler, 2005). Weather generators generate synthetic sequences of hourly weather variables by
85 using random number generators that match statistics (Ailliot et al., 2015; Mezghani and Hingray,
86 2009). Various statistical methods exist for temporal disaggregation of daily climate data, ranging from
87 simple interpolations or deterministic approaches to non-parametric approaches and methods that
88 derive statistical relationships from historical data [or look for climate analogues](#) (Bennett et al., 2020;
89 Breinl and Di Baldassarre, 2019; [Chen, 2016](#); Debele et al., 2007; Förster et al., 2016; Görner et al.,
90 2021; Liston and Elder, 2006; Park and Chung, 2020; Verfaillie et al., 2017; Poschlod et al., 2018; Zhao
91 et al., 2021). Each of these methods has its own advantages and limitations, and the choice of method
92 depends on factors such as the specific needs of the impact assessment, the quality of the available
93 data, and computational resources.

94 Here, we introduce the Teddy-Tool (**temporal disaggregation of daily climate model data**), which uses
95 statistical methods for temporal disaggregation of daily climate model data. Existing statistical
96 approaches are often only valid for a specific location and cannot be applied globally. In addition,
97 available disaggregation tools often focus on only one variable and therefore do not consider physical
98 interdependencies between different variables, such as precipitation, humidity, temperature, and
99 radiation. Teddy has been specifically developed as a globally applicable tool for climate impact
100 studies. For this purpose, Teddy strictly preserves mass and energy of daily climate model data for each
101 variable throughout the disaggregation procedure. Teddy additionally aims at taking regional and
102 seasonal climate characteristics into account and considers the physical consistency between
103 variables.

104 [Teddy](#) represents an easy-to-use tool that can be applied for climate impact assessments in different
105 sectors that allows a physically consistent temporal disaggregation of [daily climate model data](#). The

[3] nach unten verschoben: In principal, the Teddy-Tool can be used with any climate input, but has particularly been used so far with bias corrected daily CMIP6 climate data (Eyring et al., 2016) for historical time periods and future scenarios from the ISIMIP (Inter-Sectoral Impact Model Intercomparison Project), which provides bias corrected and trend-preserved climate data (Lange, 2019) and offers a framework for consistently projecting the impacts of climate change across affected sectors and spatial scales (Warszawski et al., 2014). To guarantee cross-sectoral consistency, all sectors are provided with the same climate data. Within ISIMIP, some models from different sectors have expressed their need for sub-daily climate data, including the agricultural and the energy sector.

Gelöscht: the

Gelöscht: ISIMIP

122 Teddy-Tool has been written in Matlab and is available open source via Zenodo
 123 (<https://doi.org/10.5281/zenodo.7679149>).

124 [Data and data requirements](#)

125 In principal, the Teddy-Tool can be used with any climate input, but has specifically been developed to
 126 be used with daily climate data for historical time periods and future scenarios from the Inter-Sectoral
 127 Impact Model Intercomparison Project (ISIMIP), which offers a framework for consistently projecting
 128 the impacts of climate change across affected sectors and spatial scales (Warszawski et al., 2014). To
 129 guarantee cross-sectoral consistency in ISIMIP, all sectors are provided with the same climate data.
 130 ISIMIP provides bias-corrected climate model data from the Coupled Model Intercomparison Project
 131 Phase 6 (CMIP6) and trend-preserving reanalysis climate data (Lange, 2019). Within ISIMIP, some
 132 modeling communities from different sectors have expressed their need for sub-daily climate data,
 133 including the agricultural and the energy sector.

134 Daily bias-corrected climate model data are provided by ISIMIP at 0.5° spatial resolution for air
 135 temperature (tas), humidity (hurs), shortwave radiation (rsds), longwave radiation (rls), air pressure
 136 (ps), wind speed (sfcwind), and precipitation (pr) (Lange, 2019). For air temperature, the daily
 137 maximum (tasmax) and minimum (tasmin) values are additionally provided. ISIMIP provides CMIP6
 138 data for the climate models GFDL-ESM4, IPSL-CM6A-LR, MPI-ESM1-2-HR, MRI-ESM2-0, and UKESM1-
 139 0-LL.

140 Teddy requires hourly climate data as a reference for temporal disaggregation. Therefore, we use the
 141 WFDE5 dataset, which has been generated using the WATCH Forcing Data (WFD) methodology applied
 142 to ERA5 reanalysis data (Cucchi et al., 2020). The bias-adjusted hourly WFDE5 data is globally available
 143 for the time period between 1979 and 2019 at 0.5° spatial resolution. It is consistent with the bias-
 144 adjustment procedure within ISIMIP (Lange, 2019) and thus provides a consistent hourly reference
 145 data for Teddy.

146 Table 1 gives an overview of the available variables and the required datasets at their temporal
 147 resolution. The temporal resolution of the Teddy output is adjustable by the user and can be set to 1-
 148 , 2-, 3-, 4-, 6-, 8-, or 12-hourly values.

149 Table 1: Variables and units of used hourly (h) and daily (d) climate data and the Teddy output. For
 150 WFDE5, the specific variable name is provided in brackets. WFDE5 variables have instantaneous values,
 151 while SWdown, LWdown, Rainf and Snowf have average values over the next hour at each time step.

<u>Variable</u>	<u>WFDE5 (h)</u>	<u>ISIMIP Climate Model (d)</u>	<u>Teddy (flexible)</u>
<u>tas</u>	<u>K (Tair)</u>	<u>K</u>	<u>K</u>
<u>tasmin</u>	<u>=</u>	<u>K</u>	<u>=</u>
<u>tasmax</u>	<u>=</u>	<u>K</u>	<u>=</u>
<u>hurs/huss</u>	<u>kg/kg (Qair)</u>	<u>%</u>	<u>%</u>
<u>rsds</u>	<u>W m⁻² (SWdown)</u>	<u>W m⁻²</u>	<u>W m⁻²</u>

- Formatiert:** Schriftart: Fett
- Formatiert:** Schriftart: Fett
- [3] verschoben (Einfügung)**
- Gelöscht:** particularly
- Gelöscht:** used
- Gelöscht:** so far
- Gelöscht:** bias corrected
- Gelöscht:** CMIP6
- Gelöscht:** (Eyring et al., 2016)
- Gelöscht:** ISIMIP (
- Gelöscht:** ,
- Gelöscht:** provides bias corrected and trend-preserved climate data (Lange, 2019) and
- Gelöscht:** ed
- Gelöscht:** To guarantee cross-sectoral consistency, all sectors are provided with the same climate data.
- Gelöscht:**
- [2] verschoben (Einfügung)**
- Gelöscht:** Teddy uses an empirical approach, which applies the region-specific diurnal course from the most similar day in the past to daily climate model data for a day of interest. Teddy has been developed specifically to disaggregate
- Gelöscht:** daily
- Gelöscht:** from
- Gelöscht:** the
- Gelöscht:** project
- Gelöscht:** for
- Gelöscht:** (tasmax, tasmin)
- Gelöscht:** different historical and future time periods and scenarios
- Gelöscht:** for the
- Gelöscht:**
- Gelöscht:** As a reference,
- Gelöscht:** globally available hourly bias-corrected reanalysis WFDE5 data (1980-2019) are used at 0.5° spatial resolution to identify the most similar meteorological day in the past for a specific location (Cucchi et al., 2020).
- [4] verschoben (Einfügung)**
- Formatiert:** Links
- Formatierte Tabelle**
- Formatiert:** Links
- Formatiert:** Links
- Formatiert:** Links
- Formatiert:** Links
- Formatiert:** Links

<u>rlds</u>	<u>W m⁻² (LWdown)</u>	<u>W m⁻²</u>	<u>W m⁻²</u>
<u>pr</u>	<u>kg m⁻² s⁻¹ (Rainf+Snowf)</u>	<u>kg m⁻² s⁻¹</u>	<u>mm timestep⁻¹</u>
<u>ps</u>	<u>Pa (PSurf)</u>	<u>Pa</u>	<u>hPa</u>
<u>sfcwind</u>	<u>m s⁻¹ (Wind)</u>	<u>m s⁻¹</u>	<u>m s⁻¹</u>

Formatiert: Links

Formatiert: Links

Formatiert: Links

Formatiert: Links

185

186 Methods

187 Teddy uses an empirical approach, which 1) selects the 'most similar meteorological day' for the daily
 188 climate model data (here: ISIMIP CMIP6 data) within the reference climate data (here: WFDE5) at the
 189 same location. 2) Teddy applies the location-specific diurnal course to each variable of the daily climate
 190 model data for a day of interest. In the following, the procedure is explained in detail, where the
 191 example case of ISIMIP climate data and WFDE5 reference data is used for further illustration:

192 In a first precalculation step, in order to minimize computational resources, hourly WFDE5 data are
 193 aggregated to daily values and stored as NetCDF files. The daily aggregation uses mean values for all
 194 variables and daily sums for precipitation. In addition, rainfall and snowfall fluxes must be summed
 195 up for WFDE5. Daily maximum and minimum temperature are calculated from the hourly data. Units
 196 of climate inputs are converted to match the Teddy output (see Tab. 1). For the conversion of specific
 197 humidity to relative humidity, the Buck equation is applied (Buck, 1981).

Gelöscht: ¶

Formatiert: Schriftart: Fett

Gelöscht: Temporal disaggregation¶

Gelöscht: region

Gelöscht: from the most similar meteorological day in the past

[2] nach oben verschoben: Teddy uses an empirical approach, which applies the region-specific diurnal course from the most similar day in the past to daily climate model data for a day of interest. Teddy has been developed specifically to disaggregate daily bias-corrected climate model data from the ISIMIP project at 0.5° spatial resolution for air temperature (tas), humidity (hurs), shortwave radiation (rlds), longwave radiation (rlds), air pressure (ps), windspeed (sfcwind), and precipitation (pr) (Lange, 2019). For air temperature, the daily maximum and minimum values (tasmax, tasmin) are additionally provided. ISIMIP provides data for different historical and future time periods and scenarios for the climate models GFDL-ESM4, IPSL-CM6A-LR, MPI-ESM1-2-HR, MRI-ESM2-0, and UKESM1-0-LL. As a reference, globally available hourly bias-corrected reanalysis WFDE5 data (1980-2019) are used at 0.5° spatial resolution to identify the most similar meteorological day in the past for a specific location (Cucchi et al., 2020).

Gelöscht: The diurnal profile of the most similar meteorological day is subsequently applied to the daily climate model data for each of the variables.

Gelöscht: ¶

[4] nach oben verschoben: Table 1: Variables and units of used hourly (h) and daily (d) climate data and the Teddy output. For WFDE5, the specific variable name is provided in brackets. WFDE5 variables have instantaneous values, while SWdown, LWdown, Rainf and Snowf have average values over the next hour at each time step. ¶ Variable

198 After reading the daily climate model data for the selected location (latitude/longitude) that
 199 determines a specific grid cell at 0.5° resolution, the daily mean values of all ISIMIP variables (see Tab.
 200 1) are compared to the aggregated daily values of WFDE5 for a specific time step in order to identify
 201 the most similar meteorological day. For the comparison, a day-of-year (DOY) window can be selected
 202 by the user that allows for a selection of days around the DOY of the actual time step. By default, the
 203 DOY window size is set to 11, which means a sequence of ± 11 days around the actual DOY. As a result,
 204 23 days are selected from each of the 40 WFDE5 reference years (1980-2019). These 920 days now
 205 serve as the statistical population for further calculations (Fig. 1). In a next step, the climate model day
 206 of interest and the statistical population of 920 WFDE5 days are classified according to their
 207 precipitation state. As climate models tend to produce too many days with low-intensity precipitation

Gelöscht: basic population

Gelöscht: basic population

244 called 'drizzle bias' (Chen et al., 2021), days with aggregated daily precipitation values below 1 mm per
 245 day are considered as dry days (Sun et al., 2006). Depending on the precipitation state of the previous
 246 day, the day of interest and the following day, there are eight classes: dry-dry-dry, dry-dry-wet, wet-
 247 dry-dry, wet-dry-wet, dry-wet-dry, dry-wet-wet, wet-wet-dry, and wet-wet-wet. This step is included
 248 to better reproduce the inter-day connectivity of precipitation (Li et al., 2018). Only days with the same
 249 precipitation class as the climate model day of interest are selected for the further course. Next, the
 250 absolute error between daily climate model and aggregated daily WFDE5 data for each variable is
 251 calculated for the remaining statistical population and ranked in ascending order. The ranking
 252 approach is chosen, since the absolute or relative errors of different meteorological variables cannot
 253 be compared to each other. The ranks are cumulated with equal weight over all variables for each day
 254 of the statistical population. In this context, we define 'the most similar meteorological day' as the day
 255 with the minimum sum of ranks (Fig. 1). Thus, the 'most similar meteorological day' refers to the
 256 statistical similarity of all available daily near-surface meteorological variables at a given location and
 257 time. The approach works under the assumption that similar daily values would have a similar sub-
 258 daily profile (Li et al., 2018; Pui et al., 2012; Sharma et al., 2006). Finally, the hourly values are taken
 259 from the most similar meteorological day of the WFDE5 reference dataset for each variable and are
 260 divided by the WFDE5 daily mean value of the selected day, in order to refer to relative diurnal profiles
 261 without absolute variations (Fig. 1). The hourly profile is then applied for each variable to the daily
 262 mean value from the climate model. Thus, the daily mean value of the climate model is conserved and
 263 reproduced by the disaggregated values.

264 For temperature, the resulting hourly temperature is further scaled between the provided minimum
 265 and maximum. The scaling is performed in a way that the daily mean value is preserved with an
 266 accuracy of four decimals. Relative humidity is limited to 100%, considering the preservation of the
 267 daily mean value.

268 Large selected DOY windows increase the statistical population, but on the other sight might distort
 269 climatic characteristics with a strong seasonal course such as shortwave radiation values for the actual
 270 DOY. Therefore, we preprocessed hourly potential (cloud free) solar radiation for each DOY globally at
 271 0.5° spatial resolution. This data is used as upper bound to limit the resulting hourly values for the
 272 corresponding DOY, while the daily mean value is preserved.

273 In a final step, the hourly values are aggregated to the temporal resolution as set by the user.

Gelöscht: "
 Gelöscht: "

Gelöscht: basic population

Gelöscht: over all variables

Gelöscht:

Gelöscht: basic population

Gelöscht: T

Gelöscht: is determined

Gelöscht: the lowest lowest cumulated ranks

Formatiert: Englisch (Vereinigte Staaten)

Gelöscht: '

Formatiert: Englisch (Vereinigte Staaten)

Formatiert: Englisch (Vereinigte Staaten)

Gelöscht: Hence, it does not account for the large-scale weather system at a given time step.

Gelöscht: is conserved

Gelöscht:

Gelöscht: again under

Gelöscht: preserving

Gelöscht: .

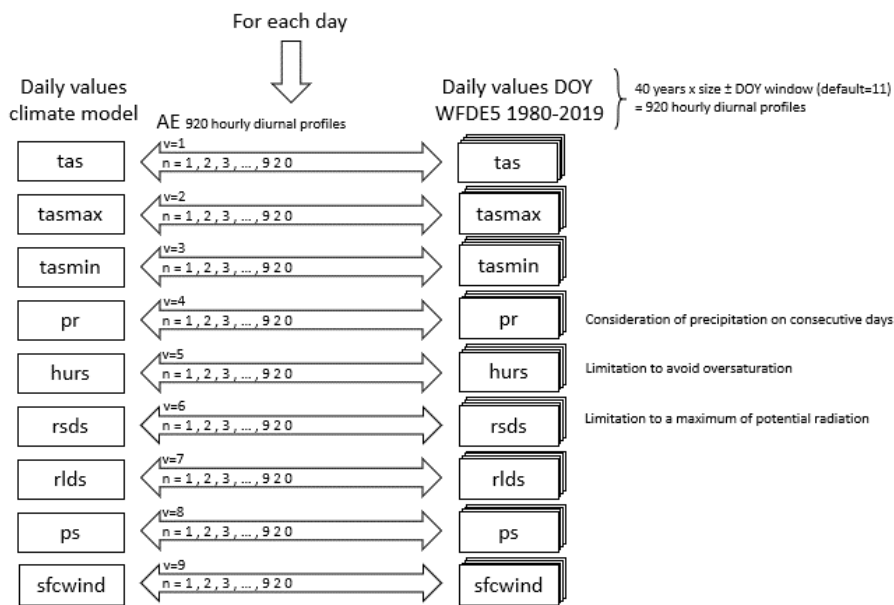
Gelöscht: basic population

Gelöscht:

Gelöscht: can again be aggregated to the time step set by the user

Gelöscht: (possible: 1, 2, 3, 4, 6, 8, 12)

Gelöscht:



297
 298 Figure 1: Procedure to identify the most similar meteorological day in the population of [WFDE5](#)
 299 reference data for the default DOY window of ± 11 days around the actual DOY.

300 In rare cases, precipitation cannot be distributed, due to [missing](#) precipitation in the reference data.
 301 [This can happen in dry deserts, where 40 years of WFDE5 data show no precipitation record within the](#)
 302 [range of the moving DOY window \(Supplementary Figure S1\).](#) To handle this exception, several options
 303 are implemented. First, the DOY window is automatically expanded to +50 days around the actual
 304 DOY [in order to increase the statistical population and thus the probability to include a precipitation](#)
 305 [event.](#) If [still no precipitation event is found in the reference](#), a linear regression between the
 306 precipitation amount and the [precipitation](#) duration is performed for the specific location across the
 307 entire [available](#) data spectrum. The linear regression determines the usual duration of the selected
 308 precipitation event. Subsequently, an hour is randomly selected for the start of the precipitation event.
 309 [A goal of Teddy was to consider the physical consistency of inter-variable relationships. Precipitation](#)
 310 [generally affects other climate variables \(e.g. humidity, radiation, temperature, etc.; Meredith et al.,](#)
 311 [2021\).](#) During night, physical interdependencies between precipitation and other variables are

- Gelöscht: failing
- Gelöscht: ?
- Formatiert: Nicht Hervorheben
- Gelöscht: see
- Gelöscht:
- Gelöscht: this doesn't help
- Formatiert: Schriftfarbe: Automatisch

317 generally lower, because radiation is not affected and less energy is available to affect other variables.
318 This might have an effect for impact models, because, as an example, evapotranspiration might be
319 unrealistically high if precipitation occurs at the same time with full solar irradiation during noon. In
320 order to reduce possible inconsistencies with other variables that could lead to implications in impact
321 models, the precipitation is only distributed to hours at nighttime. Alternatively, we implemented the
322 option for the user to write Not a Number (NaN) values instead.

323 Drizzle precipitation (values below 1 mm day⁻¹) is also disaggregated to sub-daily values in order to
324 ensure mass and energy conservation. If no historical precipitation event is found for this case,
325 precipitation noise is again randomly distributed to an hour at nighttime. If no hour without radiation
326 occurs (e.g. high latitudes in northern summer), the precipitation is distributed to local midnight.

327 The calculation procedure can be performed either for universal time (UT) or for local solar time (LST).
328 The latter divides the world into equal time zones of 15° with the central time zone (+7.5°) at
329 Greenwich.

330 Results

331 In a first step, Teddy is applied for 30 globally distributed samples (Fig. 2) for the year 2010. To be able
332 to validate the results, we perform a cross-validation. Therefore, WFDE5 data for 2010 aggregated to
333 daily values serve as an input for Teddy. The same year is excluded from the statistical population
334 during the cross-validation. As a result, it can be tested how well WFDE5 hourly values for the year
335 2010 are reproduced with the statistical population of the other 39 years. The 30 samples are chosen
336 to represent globally relevant agricultural production regions in different climate zones (Fig. 2). To
337 evaluate the sensitivity of the different DOY window sizes, we run the cross-validation with different
338 DOY window sizes, ranging from 1 to 25, in steps of two, including the option to disable the DOY
339 window (DOY window size = 0). In order to additionally validate the performance for extreme events,
340 we perform a second cross-validation for all available 40 years (1980-2019) with DOY window sizes of
341 11 and 25 for sample location 29, located in Southern Germany.

Gelöscht: physical

Gelöscht: (without solar radiation)

Gelöscht: “

Gelöscht: bias”

Gelöscht: Precipitation

Gelöscht:

Gelöscht: are

Gelöscht: l

Formatiert: Schriftart: Nicht Fett

[1] nach unten verschoben: Validation¶

Formatiert: Schriftart: Fett

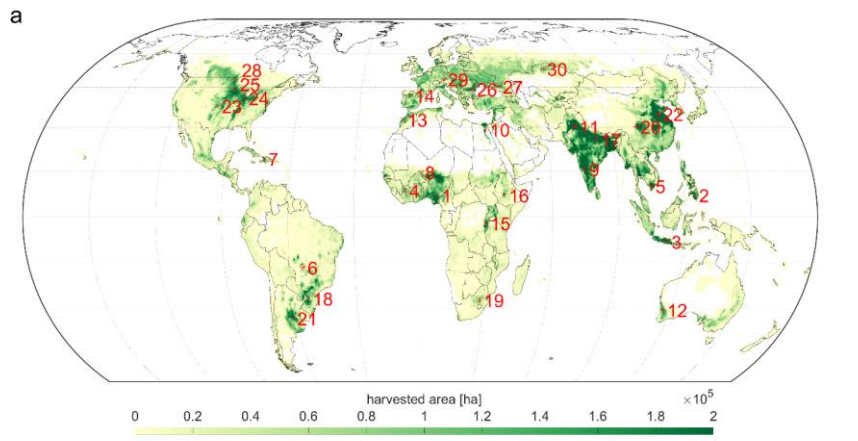
Gelöscht: In a first step, a cross-validation is carried out for 30 globally distributed samples (Fig. 2) for the year 2010.

Gelöscht: s

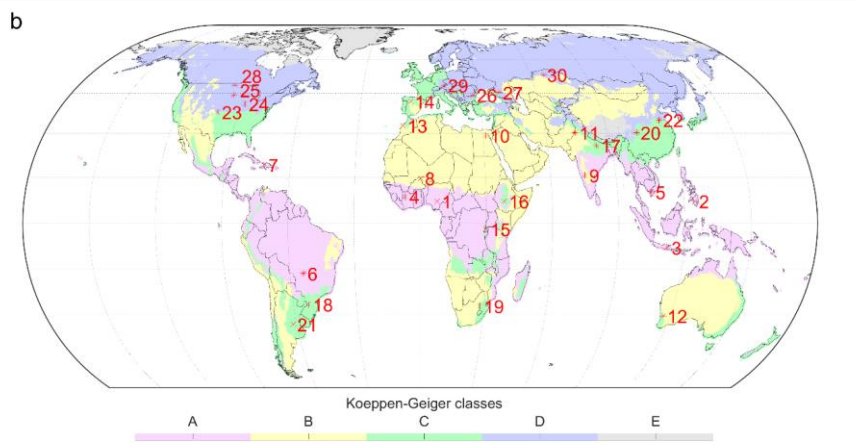
Gelöscht: basic population

Gelöscht: basic population

Gelöscht: all



357



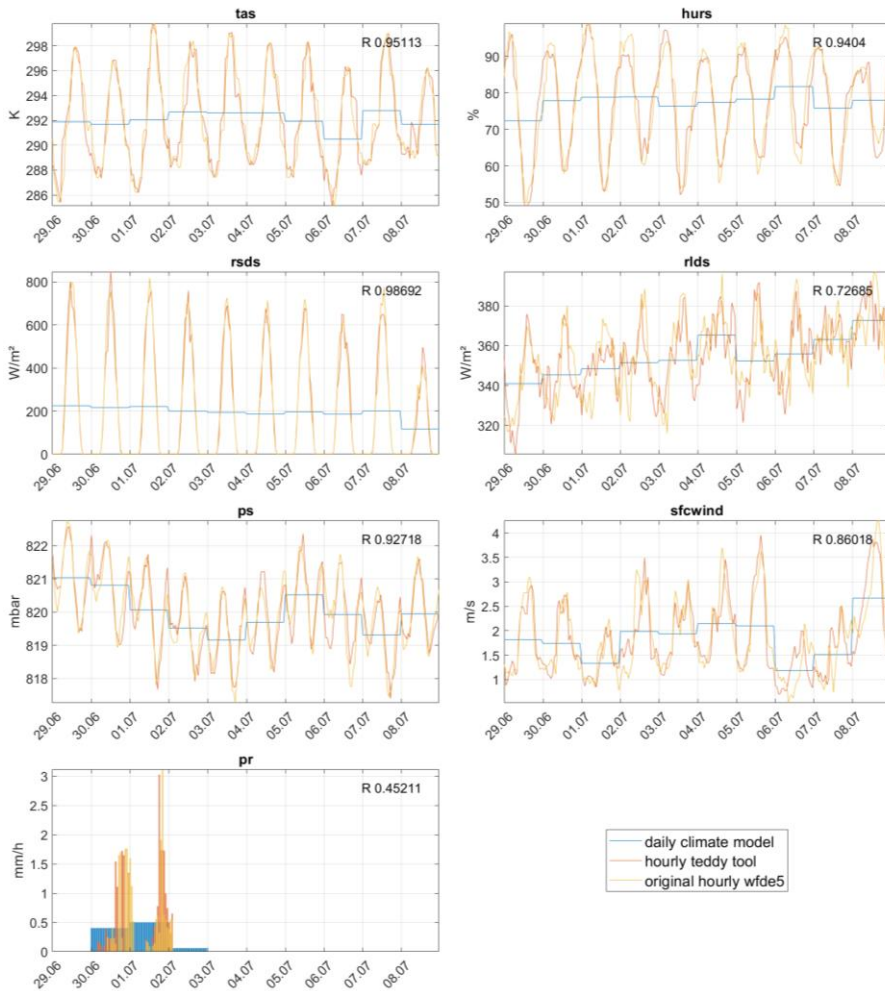
358

359 Figure 2: Distribution of 30 global samples used for the cross-validation on (a) annual total harvested
 360 area of rainfed and irrigated crops in hectare per pixel at a 30 arc-minute grid (Portmann et al., 2010)
 361 and (b) for Koeppen-Geiger climate zones calculated for 1980-2019 WFDE5 temperature and
 362 precipitation values (Beck et al., 2018). Samples are ordered by climate zone affiliation and their
 363 distance to the equator.

364 Validation

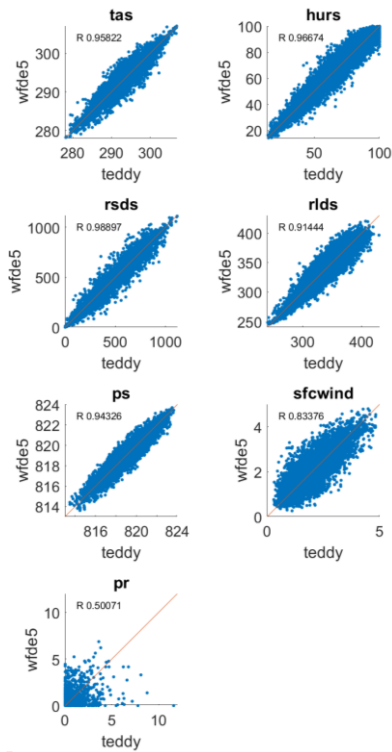
365 As an example, for sample location 16 in Ethiopia, Fig. 3 shows the results of the temporal
 366 disaggregation series for the cross-validation for a 10-day time series in 2010 in comparison with the
 367 daily climate input and the original hourly WFDE5 data. The hourly courses show high correlations for
 368 the randomly selected time series for all variables except for precipitation (Fig. 3 and scatterplots in
 369 Fig. 4 for the entire year).

[1] verschoben (Einfügung)
 Formatiert: Schriftart: Nicht Fett, Unterstrichen
 Gelöscht: example



371

372 Figure 3: Time-series for all variables comparing daily climate model data, disaggregated hourly results
 373 of Teddy from the performed cross-validation and the original hourly WFDE5 data, shown for sample
 374 location 16 in Ethiopia with a DOY window size of 7 for the 10-day period 29.06. – 08.07.2010. The
 375 Pearson correlation coefficient (R) is displayed for the shown time period for each variable.



376

377 Figure 4: Hourly values for the year 2010 between disaggregated values generated by the Teddy-Tool
 378 and the original WFDE5 data used for the cross-validation, exemplarily for sample 16 in Ethiopia with
 379 a DOY window size of 7.

380 Sensitivity analysis DOY window size

381 The sensitivity analysis averaged over all 30 samples shows that the Pearson correlation coefficient of
 382 hourly values for the year 2010 show high correlations for all variables ($r > 0.9$), except wind_speed
 383 ($r > 0.7$) and precipitation ($r > 0.4$), which are generally more difficult to disaggregate (Fig. 5). The
 384 selected DOY window size has an effect on the quality of the results. While no DOY window (size=0)
 385 results in the lowest correlation coefficient across all variables, the DOY window size does significantly
 386 affect the correlation for precipitation and wind speed (Fig. 5).

Gelöscht: ¶

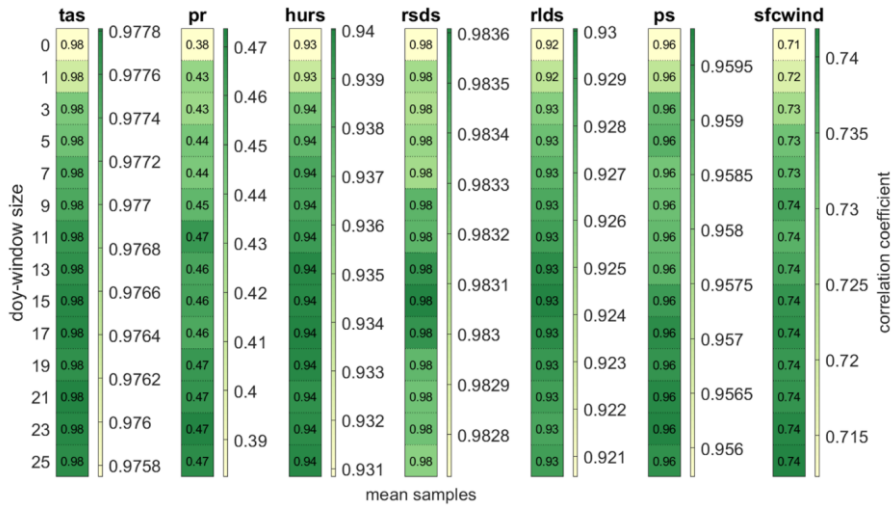
Formatiert: Unterstrichen

Formatiert: Standard, Keine Aufzählungen oder Nummerierungen

Gelöscht: are the most difficult variables for disaggregation

Gelöscht: not

Gelöscht: except

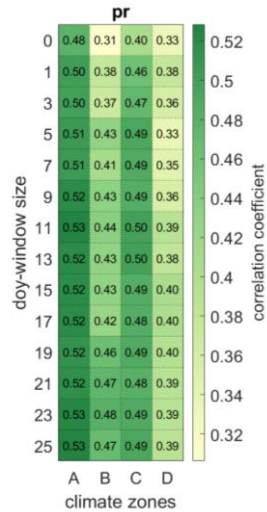


391

392 Figure 5: Pearson correlation coefficient for different DOY window sizes averaged over all 30 samples
 393 for the year 2010 for all variables being disaggregated to hourly values. The scaling of the colorbar
 394 differs between variables.

395 For precipitation, the impact of the DOY window size on the correlation varies between regions. Larger
 396 DOY windows are mainly beneficial for precipitation in arid regions, while showing lower increases in
 397 correlation in regions with pronounced seasons (Fig. 6). The results also show that the correlation for
 398 precipitation is generally larger in tropical regions than in continental regions.

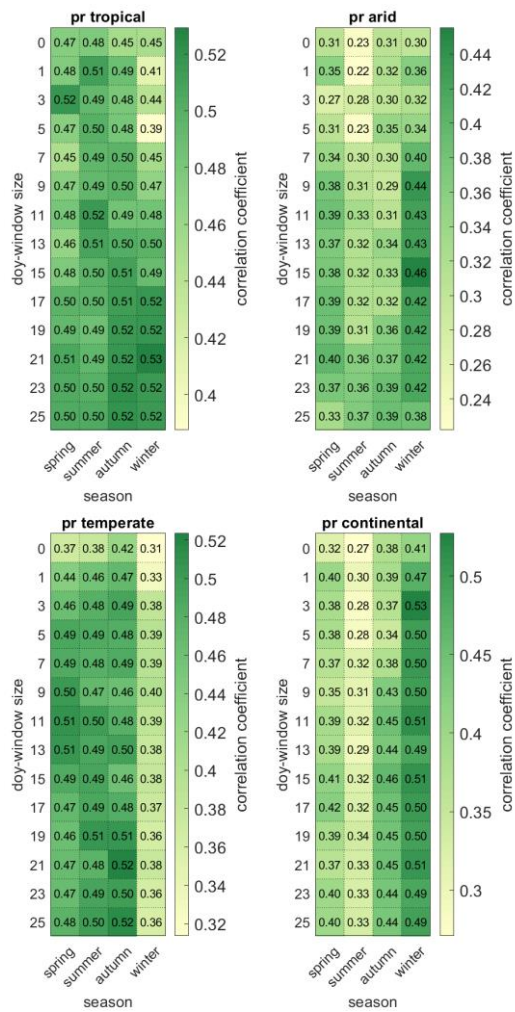
Gelöscht: tropical and
 Gelöscht: , the correlation might decrease with larger DOY window size



399

400 Figure 6: Pearson correlation coefficient for different DOY window sizes averaged over the samples for
 401 each Koepfen-Geiger climate zone (A=tropical, B=arid, C=temperate, D=continental).

405 While hourly precipitation can be best reproduced for winter seasons in continental and arid regions,
 406 winter seasons show the lowest correlation for temperate regions. Tropical regions only show
 407 relatively low variations over the year, independently from the selected DOY window size (Fig. 7).
 408 Especially in arid regions, the length of the DOY window size affects the results differently in different
 409 seasons. Here, larger DOY windows decrease the correlation during the rainy season (winter and
 410 spring), while correlation is increased during the dry season (summer and autumn).

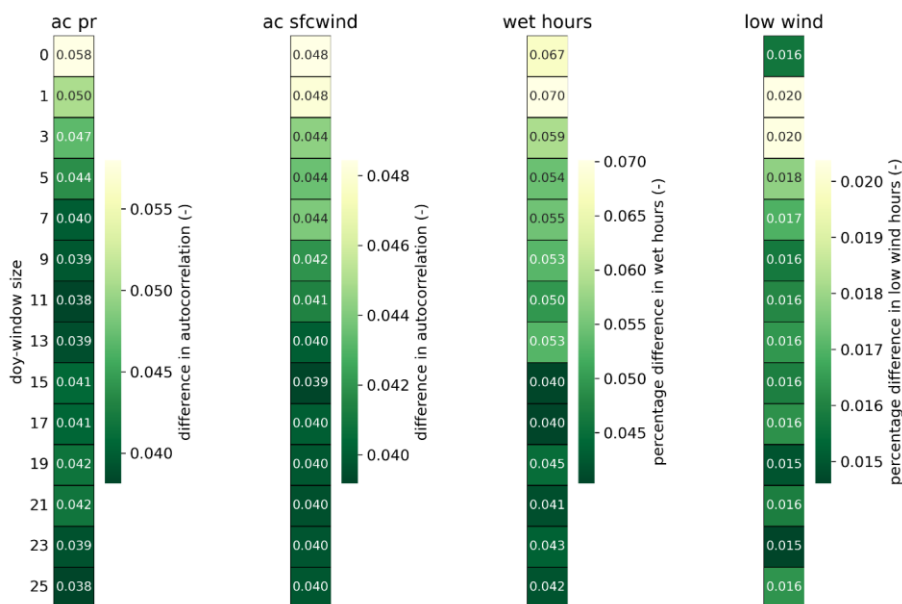


411
 412 Figure 7: Pearson correlation coefficient for different DOY window sizes averaged over the samples for
 413 the four seasons (Northern hemisphere: spring=MAM, summer=JJA, autumn=SON, winter=DJF;
 414 Southern hemisphere: spring=SON, summer=DJF, autumn= MAM, winter=JJA). The heatmap is
 415 averaged over the samples for each Koeppen-Geiger climate zone (A=tropical, B=arid, C=temperate,
 416 D=continental).

Gelöscht: The shift of the seasons between Northern and Southern hemisphere is considered.

419 Furthermore, we evaluate the sensitivity of the DOY window size to the reproduction of temporal
 420 autocorrelation (Fig. 8). Therefore, the autocorrelation over lag times between one and 24 hours is
 421 calculated for precipitation and wind speed. Autocorrelation refers to the similarity of a time series to
 422 a lag duration shifted version of the same time series. This allows sub-daily patterns and inter-hour
 423 connectivity to be statistically captured and validated in time series of precipitation and wind speed.
 424 In addition, we also check the reproduction of wet hours (precipitation above 0.1 mm h^{-1}) in 2010 and
 425 the number of hours with low wind speeds ($\text{sfcwind} < 2.5 \text{ m s}^{-1}$) referring to the typical cut-in wind
 426 speed of wind turbines.

427 Here, we find that short DOY window sizes below 5 days are not beneficial to all statistics. The
 428 autocorrelation of precipitation (wind speed) is reproduced more accurately with window sizes of 9
 429 days or longer. The number of wet hours is better recreated with window sizes above 15 days. For
 430 hours with low wind speed, a minor improvement is found above 9 days.



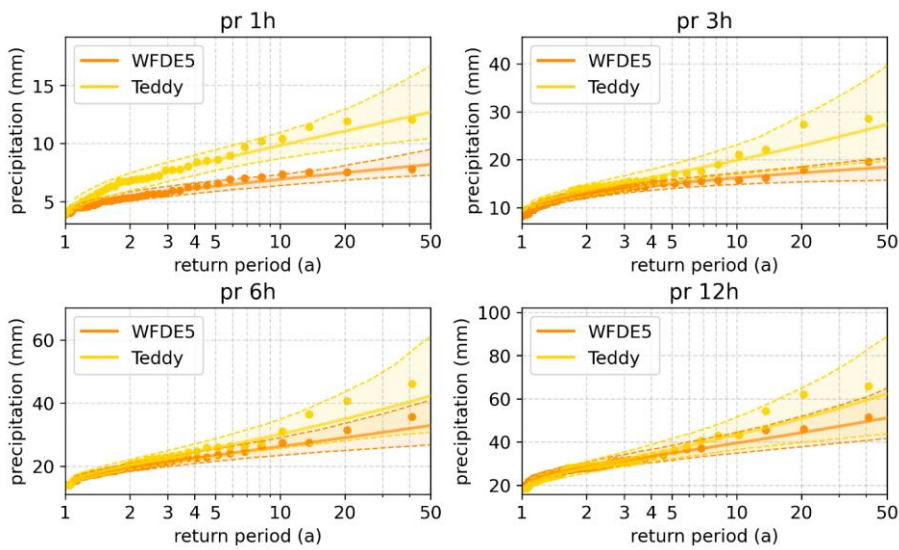
431
 432 Figure 8: Extended validation statistics for the sensitivity analysis of the DOY window size for the year
 433 2010. The difference in autocorrelation refers to the average over all 30 stations and lag durations
 434 between one and 24 hours. Wet hours are defined as precipitation intensities above 0.1 mm h^{-1} , and
 435 low wind speeds refer to hours with $\text{sfcwind} < 2.5 \text{ m s}^{-1}$.

Gelöscht: mm h^{-1}

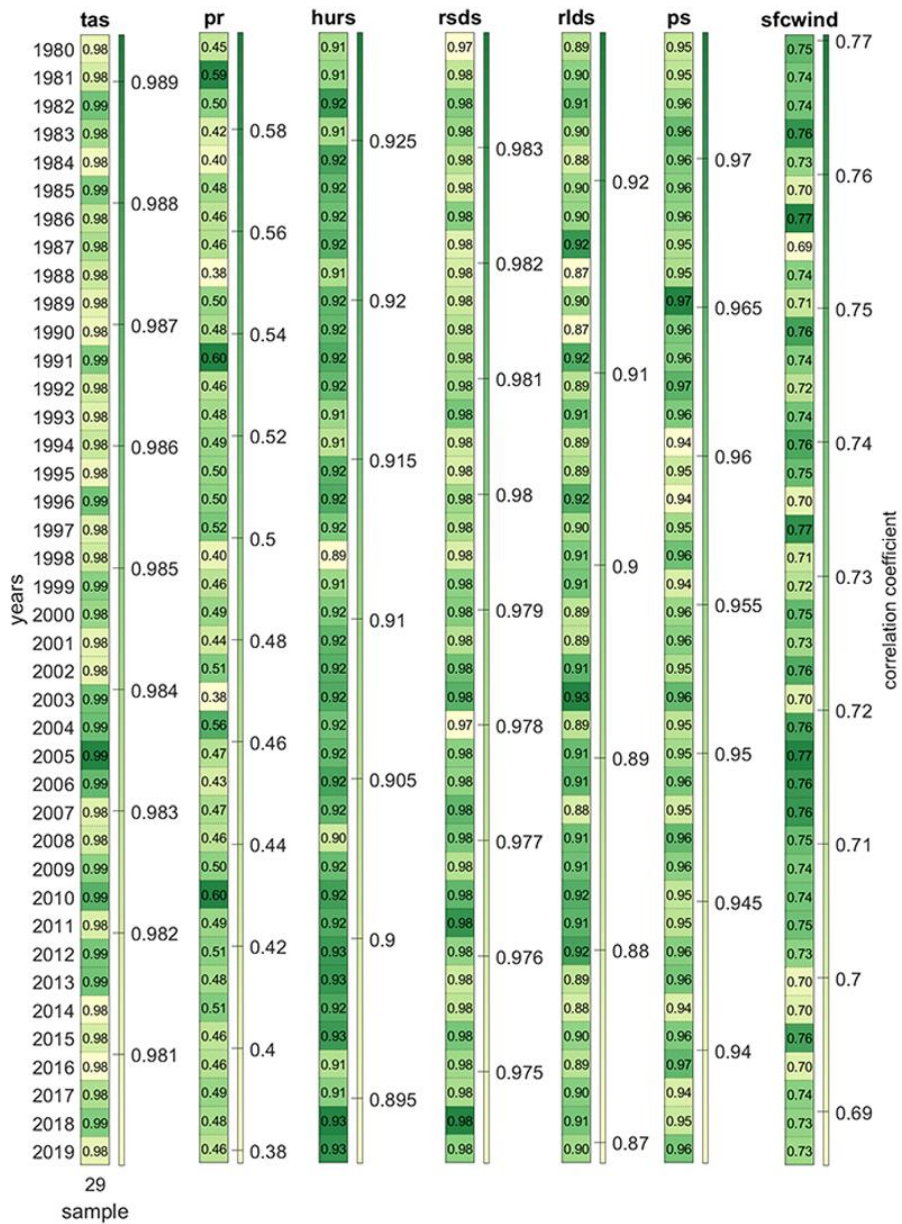
Gelöscht: m s^{-1}

436 As the ISIMIP data base is used for future impact modelling and historical attribution science (Mengel
 437 et al., 2021), extremes are of major interest for the community. The ability of global climate models to
 438 simulate sub-daily extremes is limited and depends on the variable of interest and the spatio-temporal
 439 conditions of the extreme and the respective model setup (Wehner et al., 2021; Kumar et al., 2015;
 440 Wang and Clow, 2020). However, in this validation, we need to evaluate how the Teddy-Tool is able to
 441 preserve the statistics of sub-daily extreme values. Therefore, we select precipitation as variable of
 442 interest. Figure 9 shows the reproduction of sub-daily precipitation extremes for 1980 – 2019 for

445 sample location 29 in southern Germany, where Teddy is run with a DOY window size of 11 days. The
 446 40 annual maxima are extracted from the original and the disaggregated data. Additionally, the
 447 Generalized Extreme Value (GEV) distribution is fitted to these empirical data. Thereby, 95%
 448 confidence intervals are generated applying a bootstrap procedure with 1000 iterations to account for
 449 extreme value statistical uncertainties. We find that the Teddy-Tool leads to an overestimation of
 450 annual maximum precipitation. For the hourly duration, the differences are large with the confidence
 451 intervals of the GEV hardly overlapping. For the longer durations, Teddy values approach the original
 452 data, with noticeable differences only for the rare events with return periods above 5 years.



453
 454 Figure 9: Extreme value statistical evaluation of sub-daily precipitation. The annual maxima of the
 455 WFDE5 and Teddy are shown as dots. Additionally, GEV fits (lines) with 95% confidence intervals
 456 (transparent areas and dashed lines) account for uncertainties. The Teddy-Tool is run with a DOY
 457 window size of 11 days.



458

459 Figure 10: Pearson correlation coefficient for each year for sample location 29 and a DOY window size
 460 of 11 days. The scaling of the colorbar differs between variables.

461 [Discussion and Outlook](#)

Formatiert: Schriftart: Fett

Formatiert: Standard, Keine Aufzählungen oder Nummerierungen

Gelöscht: Conclusions

Formatiert: Schriftart: Fett

463 The Teddy-Tool allows for temporal disaggregation of daily climate model data. The disaggregation is
464 based on location and time specific empirical relationships between variables. The approach is well
465 suitable for all tested variables and results in very high correlations (>0.9), except for precipitation
466 (>0.5) and wind speed (>0.75). We refer the worse performance for precipitation and wind speed to
467 the high intra-day variability for these variables (Watters et al., 2021). Other variables are governed by
468 a stronger diurnal cycle (Dai and Trenberth, 2004), which is easier to disaggregate based on empirical
469 diurnal profiles.

Gelöscht: er

Gelöscht: The o

470 Compared to other approaches, the advantage of the Teddy-Tool is that no other input data is required
471 rather than the daily climate model data. The Teddy-Tool is relatively simple to apply, considers specific
472 local and seasonal features of the diurnal course of different climate variables, and preserves the
473 physical consistency of inter-variable relationships. Mass and energy are conserved and mean daily
474 values of the climate model are reproduced any time.

Gelöscht: regional

Gelöscht: considers

Gelöscht:

475 The spatial and temporal resolution of the results is determined by the provided temporal and spatial
476 resolution of the chosen reference data (WFDE5 used here). Longer available reanalysis time periods
477 extend the statistical population for identifying the most similar weather conditions in the past and
478 thus could improve the results. Generally, also other reference data could be used, that provides higher
479 temporal or spatial resolution for a specific region.

Gelöscht: basic population

480 The DOY window to find the most similar historical weather situations can be chosen in different sizes.
481 For most of the variables, we found small effects of time window adjustments, except for precipitation
482 and wind speed. The evaluation of different DOY window sizes reveals that a DOY window size of 11
483 can generally be recommended across all variables. Larger DOY windows should be avoided mainly in
484 arid regions, while shorter DOY windows generally lead to poorer representations of autocorrelation
485 and extreme events.

Gelöscht: time

Gelöscht:

486 One limitation of the Teddy-Tool is the representation of extreme events, mainly for precipitation,
487 which is generally the most difficult variable for temporal disaggregation. We found that hourly
488 precipitation extremes are overestimated. For heavy daily precipitation events, Teddy distributes the
489 24h-sums either correctly, too evenly or on too few hours. When distributing on too few hours,
490 extreme hourly intensities evolve, which may have never occurred or may even be physically
491 implausible. For temporal disaggregation of extreme precipitation, we recommend dynamical
492 downscaling via high-resolution climate models (Poschlod, 2021; Poschlod et al., 2021; Zabel et al.,
493 2012; Zabel and Mauser, 2013).

Gelöscht: not always reproduced

Gelöscht:

494 Another limitation of the approach is the reproduction of the inter-day connectivity within the
495 disaggregated time series. When two diurnal profiles are chosen for the disaggregation of adjacent
496 days, which show dissimilar courses in the time steps at the change of the day, abrupt value jumps
497 might occur in the disaggregation. This can be seen in Fig. 3 for rlds from July 4th to July 5th. To illustrate
498 this issue, a disaggregation time series from another location is provided in Supplementary Figure S2.
499 This limitation does also apply for the Method of Fragments applied on precipitation (Li et al., 2018).
500 Similarly to Li et al. (2018), we also consider the precipitation state of the previous and following day
501 to improve inter-day connectivity. Without this additional consideration, overnight precipitation
502 events would often be 'cut off' in the disaggregation. For the remaining abrupt jumps in the
503 disaggregated time series, we refrain from post-processing with subsequent smoothing, as we want to
504 preserve both mass and energy and the empirical diurnal profiles.

Gelöscht: 4

Formatiert: Hochgestellt

Gelöscht: 5

Formatiert: Hochgestellt

Gelöscht: the

Gelöscht: "

Gelöscht: "

Gelöscht:

521 For the disaggregation of future climate projections using of the Teddy-Tool, we have the following
 522 remarks: As the Teddy-Tool derives the relationships between sub-daily and daily values empirically
 523 based on reanalysis data, future diurnal profiles, which are outside the historical range of diurnal
 524 profiles, might possibly be not fully reproduced. However, this limitation is common for statistical
 525 approaches, which are to be calibrated on historical data (Papalexiou et al., 2018). Nevertheless, due
 526 to energy and mass conservation, climate trends in the daily climate signal are fully preserved. Hence,
 527 applying Teddy for temporal disaggregation under climate change holds under the assumption that we
 528 select the most similar meteorological day of the historical data and that this diurnal profile is
 529 representative for future climatic conditions. However, this assumption might apply to a different
 530 degree for different variables. We expect non-stationarity for the diurnal profiles due to changing
 531 weather patterns, shifts in rainfall generating processes, and shifts in the seasonality, mainly for
 532 precipitation and wind. The daily course of other variables, such as solar radiation and temperature
 533 might generally be less affected by a warmer climate. Furthermore, global climate models at coarse
 534 resolutions generally do not represent all processes to fully reproduce intra-day variability. Teddy
 535 applies the diurnal profiles and intra-day variability from the WFDE5 data, which are bias-adjusted
 536 ERA5 reanalysis data that implicitly consider finer scale effects than coarse-resolution global climate
 537 models (Cucchi et al., 2020). Thus, the disaggregation process in Teddy is consistent with the bias
 538 adjustment in ISIMIP3.

539 Another limitation of the methodology could occur in the case of strong climate change signals. In case
 540 of high warming in end-of-century projections, the number of sampled historical days might decrease
 541 if the same historical day is sampled repeatedly. This could lead to reductions in diversity of the diurnal
 542 profile. Hence, Teddy allows to monitor the number of unique analogue days per year. An additional
 543 analysis for SSP3-7.0 using the GFDL-ESM4 climate model shows that the number of unique analogue
 544 climate days are declining, as expected, but still the diversity of chosen days is above 300 unique days
 545 at the end of the century for a chosen moving-window size of ± 11 days (Supplementary Fig. S3). A
 546 smaller size of the moving window prevents that the same analogue day is chosen over a longer time
 547 period. This will increase the diversity of diurnal profiles at the expense of similarity. Even if diurnal
 548 profiles are derived from the same analogue day repeatedly, the disaggregated diurnal courses, e.g.
 549 for temperature, will show variations (different offset and different amplitude) due to conservation of
 550 daily mean energy and mass. From a broader perspective, it is also not clear whether the uncertainties
 551 resulting from this limitation are larger than the uncertainties within the climate model projections
 552 until the end of the century. Furthermore, in the long term, the basic population for finding analogue
 553 climates will continuously increase, since WFDE5 data, which are based on ERA5, are continuously
 554 updated. We note that Teddy could be also employed to disaggregate future daily climate projections
 555 based on hourly future climate projections as reference.

556 Further possible developments could include improvements for the reproduction of the inter-day
 557 connectivity. Despite the consideration of precipitation classes, still abrupt value jumps over day
 558 changes are possible. A future introduction of temperature classes and surface pressure classes in
 559 addition to the precipitation classes could help to reduce this effect. Depending on the location of
 560 interest, also including climate modes or weather patterns for the choice of the most similar
 561 meteorological day could positively affect the performance. Furthermore, depending on the
 562 application, it could be reasonable not to screen for the most similar meteorological day, but for the
 563 most similar succession of multiple days. This would as a consequence improve the inter-day
 564 connectivity as less different profiles are selected.

- Formatiert:** Standard
- Gelöscht:** In order to prevent for high warming
- Formatiert:** Nicht Hervorheben
- Formatiert:** Nicht Hervorheben
- Gelöscht:** that
- Gelöscht:** , which
- Formatiert:** Nicht Hervorheben
- Formatiert:** Nicht Hervorheben
- Formatiert:** Nicht Hervorheben
- Formatiert:** Nicht Hervorheben
- Gelöscht:**
- Formatiert:** Nicht Hervorheben
- Formatiert:** Nicht Hervorheben
- Formatiert:** Nicht Hervorheben
- Formatiert:** Schriftfarbe: Automatisch
- Gelöscht:** Since mass and energy are conserved within the disaggregation approach, the
- Gelöscht:** might
- Gelöscht:** despite the diurnal profile are derived from the same analogue day
- Gelöscht:**
- Gelöscht:** an improved
- Gelöscht:** changes
- Gelöscht:** improve

578 Other optional future developments could include the separation of direct and diffuse radiation, which
579 is also a required information for some impact models which is currently not provided by ISIMIP.
580 However, we would make further development with more options dependent on the community's
581 adoption of the current executable tool.

582 **Code availability**

583 The source code of the Teddy-Tool (v1.0) and a parallelized version of the Teddy-Tool (v1.0p), including
584 a precompiled executable file for Windows, preprocessed data, results of the cross-validation and
585 exemplary results for SSP 585 (2015 – 2100) and the UKESM1-0-L climate model for 30 samples are
586 provided via Zenodo (<https://doi.org/10.5281/zenodo.7679149>).

587 **Author contribution**

588 FZ: Conceptualization, Software, Methodology, Validation, Formal analysis, Resources, Data curation,
589 Writing - original draft, Visualization

590 BP: Methodology, Validation, Formal analysis, Writing - original draft, Visualization

591 **Competing interests**

592 The contact author has declared that none of the authors has any competing interests.

593 **Acknowledgements**

594 We acknowledge the methodological discussion with Stefan Lange from the Potsdam Institute of
595 Climate Impact Research (PIK).

596 **References**

- 597 Alliot, P., Allard, D., Monbet, V., and Naveau, P.: Stochastic weather generators: an overview of
598 weather type models, *Journal de la société française de statistique*, 156, <https://doi.org/101-113>,
599 2015.
- 600 Beck, H. E., Zimmermann, N. E., McVicar, T. R., Vergopolan, N., Berg, A., and Wood, E. F.: Present and
601 future Köppen-Geiger climate classification maps at 1-km resolution, *Scientific Data*, 5, 180214,
602 <https://doi.org/10.1038/sdata.2018.214>, 2018.
- 603 Bennett, A., Hamman, J. & Nijssen, B.: MetSim: A python package for estimation and disaggregation
604 of meteorological data, *Journal of Open Source Software*, 5(47), 2042,
605 <https://doi.org/10.21105/joss.02042>, 2020.
- 606 Breinl, K. and Di Baldassarre, G.: Space-time disaggregation of precipitation and temperature across
607 different climates and spatial scales, *Journal of Hydrology: Regional Studies*, 21, 126-146,
608 <https://doi.org/10.1016/j.ejrh.2018.12.002>, 2019.
- 609 Buck, A. L.: New Equations for Computing Vapor Pressure and Enhancement Factor, *Journal of*
610 *Applied Meteorology and Climatology*, 20, 1527-1532, [https://doi.org/10.1175/1520-0450\(1981\)020<1527:Nefcvp>2.0.Co;2](https://doi.org/10.1175/1520-0450(1981)020<1527:Nefcvp>2.0.Co;2), 1981.
- 612 Byers, E., Gidden, M., Leclère, D., Balkovic, J., Burek, P., Ebi, K., Greve, P., Grey, D., Havlik, P., Hillers,
613 A., Johnson, N., Kahil, T., Krey, V., Langan, S., Nakicenovic, N., Novak, R., Obersteiner, M.,
614 Pachauri, S., Palazzo, A., Parkinson, S., Rao, N. D., Rogelj, J., Satoh, Y., Wada, Y., Willaarts, B., and
615 Riahi, K.: Global exposure and vulnerability to multi-sector development and climate change
616 hotspots, *Environmental Research Letters*, 13, 055012, <https://doi.org/10.1088/1748-9326/aabf45>, 2018.

Formatiert: Block

Formatiert: Absatz-Standardschriftart

618 Chen, D., Dai, A., and Hall, A.: The Convective-To-Total Precipitation Ratio and the “Drizzling” Bias in
619 Climate Models, *Journal of Geophysical Research: Atmospheres*, 126, e2020JD034198,
620 <https://doi.org/10.1029/2020JD034198>, 2021.

621 [Chen, C. J.: Temporal disaggregation of seasonal forecasting for streamflow simulation. *World*
622 *Environmental and Water Resources Congress 2016*, pp. 63-72, 2016.](#)

623 Colón-González, F. J., Sewe, M. O., Tompkins, A. M., Sjödin, H., Casallas, A., Rocklöv, J., Caminade, C.,
624 and Lowe, R.: Projecting the risk of mosquito-borne diseases in a warmer and more populated
625 world: a multi-model, multi-scenario intercomparison modelling study, *The Lancet Planetary*
626 *Health*, 5, e404-e414, [https://doi.org/10.1016/S2542-5196\(21\)00132-7](https://doi.org/10.1016/S2542-5196(21)00132-7), 2021.

627 Cucchi, M., Weedon, G. P., Amici, A., Bellouin, N., Lange, S., Müller Schmied, H., Hersbach, H., and
628 Buontempo, C.: WFDE5: bias-adjusted ERA5 reanalysis data for impact studies, *Earth Syst. Sci.*
629 *Data*, 12, 2097-2120, <https://doi.org/10.5194/essd-12-2097-2020>, 2020.

630 [Dai, A. and Trenberth, K. E.: The Diurnal Cycle and Its Depiction in the Community Climate System
631 *Model. Journal of Climate*, 17, 930-951, \[https://doi.org/10.1175/1520-
632 0442\\(2004\\)017<0930:TDCAID>2.0.CO;2\]\(https://doi.org/10.1175/1520-

632 0442\(2004\)017<0930:TDCAID>2.0.CO;2\), 2004.](#)

633 Debele, B., Srinivasan, R., and Yves Parlange, J.: Accuracy evaluation of weather data generation and
634 disaggregation methods at finer timescales, *Advances in Water Resources*, 30, 1286-1300,
635 <https://doi.org/10.1016/j.advwatres.2006.11.009>, 2007.

636 Degife, A. W., Zabel, F., and Mauser, W.: Climate change impacts on potential maize yields in
637 Gambella region, Ethiopia, *Regional Environmental Change*, [https://doi.org/10.1007/s10113-021-
638 01773-3](https://doi.org/10.1007/s10113-021-

638 01773-3), 2021.

639 Eyring, V., Bony, S., Meehl, G. A., Senior, C. A., Stevens, B., Stouffer, R. J., and Taylor, K. E.: Overview
640 of the Coupled Model Intercomparison Project Phase 6 (CMIP6) experimental design and
641 organization, *Geosci. Model Dev.*, 9, 1937-1958, <https://doi.org/10.5194/gmd-9-1937-2016>, 2016.

642 Förster, K., Hanzer, F., Winter, B., Marke, T., and Strasser, U.: An open-source MEteoroLOgical
643 observation time series DISaggregation Tool (MELODIST v0.1.1), *Geosci. Model Dev.*, 9, 2315-
644 2333, <https://doi.org/10.5194/gmd-9-2315-2016>, 2016.

645 Franke, J. A., Müller, C., Minoli, S., Elliott, J., Folberth, C., Gardner, C., Hank, T., Izaurralde, R. C.,
646 Jägermeyr, J., Jones, C. D., Liu, W., Olin, S., Pugh, T. A. M., Ruane, A. C., Stephens, H., Zabel, F., and
647 Moyer, E. J.: Agricultural breadbaskets shift poleward given adaptive farmer behavior under
648 climate change, *Global Change Biol.*, 28, 167-181, <https://doi.org/10.1111/gcb.15868>, 2022.

649 Golub, M., Thiery, W., Marcé, R., Pierson, D., Vanderkelen, I., Mercado-Bettin, D., Woolway, R. I.,
650 Grant, L., Jennings, E., Kraemer, B. M., Schewe, J., Zhao, F., Frieler, K., Mengel, M., Bogomolov, V.
651 Y., Bouffard, D., Côté, M., Couture, R. M., Debolskiy, A. V., Droppers, B., Gal, G., Guo, M., Janssen,
652 A. B. G., Kirillin, G., Ladwig, R., Magee, M., Moore, T., Perroud, M., Piccolroaz, S., Raaman Vinnaa,
653 L., Schmid, M., Shatwell, T., Stepanenko, V. M., Tan, Z., Woodward, B., Yao, H., Adrian, R., Allan,
654 M., Anneville, O., Arvola, L., Atkins, K., Boegman, L., Carey, C., Christianson, K., de Eyto, E.,
655 DeGasperi, C., Grechushnikova, M., Hejzlar, J., Joehnk, K., Jones, I. D., Laas, A., Mackay, E. B.,
656 Mammarella, I., Markensten, H., McBride, C., Özkundakci, D., Potes, M., Rinke, K., Robertson, D.,
657 Rusak, J. A., Salgado, R., van der Linden, L., Verburg, P., Wain, D., Ward, N. K., Wollrab, S., and
658 Zdrovennova, G.: A framework for ensemble modelling of climate change impacts on lakes
659 worldwide: the ISIMIP Lake Sector, *Geosci. Model Dev.*, 15, <https://doi.org/4597-4623>,
660 10.5194/gmd-15-4597-2022, 2022.

661 Görner, C., Franke, J., Kronenberg, R., Hellmuth, O., and Bernhofer, C.: Multivariate non-parametric
662 Euclidean distance model for hourly disaggregation of daily climate data, *Theoretical and Applied*
663 *Climatology*, 143, 241-265, <https://doi.org/10.1007/s00704-020-03426-7>, 2021.

664 Jägermeyr, J., Müller, C., Ruane, A. C., Elliott, J., Balkovic, J., Castillo, O., Faye, B., Foster, I., Folberth,
665 C., Franke, J. A., Fuchs, K., Guarin, J. R., Heinke, J., Hoogenboom, G., Iizumi, T., Jain, A. K., Kelly, D.,
666 Khabarou, N., Lange, S., Lin, T.-S., Liu, W., Mialyk, O., Minoli, S., Moyer, E. J., Okada, M., Phillips,
667 M., Porter, C., Rabin, S. S., Scheer, C., Schneider, J. M., Schyns, J. F., Skalsky, R., Smerald, A., Stella,
668 T., Stephens, H., Webber, H., Zabel, F., and Rosenzweig, C.: Climate impacts on global agriculture

Formatiert: Absatz-Standardschriftart

669 emerge earlier in new generation of climate and crop models, *Nature Food*, 2, 873-885,
670 <https://doi.org/10.1038/s43016-021-00400-y>, 2021.

671 Kumar, D., Mishra, V., and Ganguly, A. R.: Evaluating wind extremes in CMIP5 climate models,
672 *Climate Dynamics*, 45, 441-453, <https://doi.org/10.1007/s00382-014-2306-2>, 2015.

673 Kunstmann, H. and Stadler, C.: High resolution distributed atmospheric-hydrological modelling for
674 Alpine catchments, *Journal of Hydrology*, 314, 105-124,
675 <https://doi.org/10.1016/j.jhydrol.2005.03.033>, 2005.

676 Lange, S.: Trend-preserving bias adjustment and statistical downscaling with ISIMIP3BASD (v1.0),
677 *Geosci. Model Dev.*, 12, 3055-3070, <https://doi.org/10.5194/gmd-12-3055-2019>, 2019.

678 Li, X., Meshgi, A., Wang, X., Zhang, J., Tay, S. H. X., Pijcke, G., Manocha, N., Ong, M., Nguyen, M. T.,
679 and Babovic, V.: Three resampling approaches based on method of fragments for daily-to-subdaily
680 precipitation disaggregation, *International Journal of Climatology*, 38, e1119-e1138,
681 <https://doi.org/10.1002/joc.5438>, 2018.

682 Liston, G. E. and Elder, K.: A Meteorological Distribution System for High-Resolution Terrestrial
683 Modeling (MicroMet), *Journal of Hydrometeorology*, 7, 217-234,
684 <https://doi.org/10.1175/jhm486.1>, 2006.

685 Liu, C., Ikeda, K., Thompson, G., Rasmussen, R., and Dudhia, J.: High-Resolution Simulations of
686 Wintertime Precipitation in the Colorado Headwaters Region: Sensitivity to Physics
687 Parameterizations, *Monthly Weather Review*, 139, 3533-3553, <https://doi.org/10.1175/MWR-D-11-00009.1>, 2011.

689 Mengel, M., Treu, S., Lange, S., and Frieler, K.: ATTRICI v1.1 – counterfactual climate for impact
690 attribution, *Geosci. Model Dev.*, 14, 5269-5284, <https://doi.org/10.5194/gmd-14-5269-2021>,
691 2021.

692 [Meredith, E., Ulbrich, U., Rust, H. W., and Truhetz, H.: Present and future diurnal hourly precipitation
693 in 0.11° EURO-CORDEX models and at convection-permitting resolution, *Environmental Research
694 Communications*, 3, 055002, <https://doi.org/10.1088/2515-7620/abf15e>, 2021.](#)

695 Mezghani, A. and Hingray, B.: A combined downscaling-disaggregation weather generator for
696 stochastic generation of multisite hourly weather variables over complex terrain: Development
697 and multi-scale validation for the Upper Rhone River basin, *Journal of Hydrology*, 377, 245-260,
698 <https://doi.org/10.1016/j.jhydrol.2009.08.033>, 2009.

699 Minoli, S., Jägermeyr, J., Asseng, S., Urfels, A., and Müller, C.: Global crop yields can be lifted by
700 timely adaptation of growing periods to climate change, *Nature Communications*, 13, 7079,
701 <https://doi.org/10.1038/s41467-022-34411-5>, 2022.

702 Orlov, A., Daloz, A. S., Sillmann, J., Thiery, W., Douzal, C., Lejeune, Q., and Schleussner, C.: Global
703 Economic Responses to Heat Stress Impacts on Worker Productivity in Crop Production,
704 *Economics of Disasters and Climate Change*, 5, 367-390, <https://doi.org/10.1007/s41885-021-00091-6>, 2021.

706 Orlov, A., et al.: Human heat stress could offset economic benefits of the CO2 fertilisation effect in
707 crop production. *Nature Communications: Under Review*, 2023.

708 Papalexiou, S. M., Markonis, Y., Lombardo, F., AghaKouchak, A., and Foufoula-Georgiou, E.: Precise
709 Temporal Disaggregation Preserving Marginals and Correlations (DiPMaC) for Stationary and
710 Nonstationary Processes, *Water Resources Research*, 54, 7435-7458,
711 <https://doi.org/10.1029/2018WR022726>, 2018.

712 Park, H. and Chung, G.: A Nonparametric Stochastic Approach for Disaggregation of Daily to Hourly
713 Rainfall Using 3-Day Rainfall Patterns, *Water*, 12, 2306, 2020.

714 Portmann, F. T., Siebert, S., and Döll, P.: MIRCA2000—Global monthly irrigated and rainfed crop
715 areas around the year 2000: A new high-resolution data set for agricultural and hydrological
716 modeling, *Global Biogeochemical Cycles*, 24, <https://doi.org/10.1029/2008GB003435>, 2010.

717 Poschlod, B.: Using high-resolution regional climate models to estimate return levels of daily extreme
718 precipitation over Bavaria, *Nat. Hazards Earth Syst. Sci.*, 21, 3573-3598,
719 <https://doi.org/10.5194/nhess-21-3573-2021>, 2021.

Kommentiert [ZF1]: Currently still under review.

720 [Poschlod, B.: Attributing heavy rainfall event in Berchtesgadener Land to recent climate change –](#)
721 [Further rainfall intensification projected for the future, *Weather Clim Extremes*, 38, 100492,](#)
722 <https://doi.org/10.1016/j.wace.2022.100492>, 2022.

723 Poschlod, B. and Ludwig, R.: Internal variability and temperature scaling of future sub-daily rainfall
724 return levels over Europe, *Environmental Research Letters*, 16, 064097,
725 <https://doi.org/10.1088/1748-9326/ac0849>, 2021.

726 Poschlod, B., Ludwig, R., and Sillmann, J.: Ten-year return levels of sub-daily extreme precipitation
727 over Europe, *Earth Syst. Sci. Data*, 13, 983-1003, <https://doi.org/10.5194/essd-13-983-2021>, 2021.

728 Poschlod, B., Hodnebrog, Ø., Wood, R. R., Alterskjær, K., Ludwig, R., Myhre, G., and Sillmann, J.:
729 Comparison and Evaluation of Statistical Rainfall Disaggregation and High-Resolution Dynamical
730 Downscaling over Complex Terrain, *Journal of Hydrometeorology*, 19, 1973-1982,
731 <https://doi.org/10.1175/jhm-d-18-0132.1>, 2018.

732 [Pui, A., Sharma, A., Mehrotra, R., Sivakumar, B., and Jeremiah, E.: A comparison of alternatives for](#)
733 [daily to sub-daily rainfall disaggregation, *J. Hydrol.*, 470, 138– 157,](#)
734 <https://doi.org/10.1016/j.jhydrol.2012.08.041>, 2012.

735 Reed, C., Anderson, W., Kruczkiewicz, A., Nakamura, J., Gallo, D., Seager, R., and McDermid, S. S.: The
736 impact of flooding on food security across Africa, *Proceedings of the National Academy of*
737 *Sciences*, 119, e2119399119, <https://doi.org/10.1073/pnas.2119399119>, 2022.

738 [Sharma, A. and Srikanthan, S.: Continuous Rainfall Simulation: A Nonparametric Alternative, in:](#)
739 [30th Hydrology & Water Resources Symposium: Past, Present & Future, 4–7 December 2006,](#)
740 [Launceston, Tasmania, p. 86, 2006.](#)

741 Sun, Y., Solomon, S., Dai, A., and Portmann, R. W.: How Often Does It Rain?, *Journal of Climate*, 19,
742 <https://doi.org/916-934>, 10.1175/jcli3672.1, 2006.

743 Tittensor, D. P., Novaglio, C., Harrison, C. S., Heneghan, R. F., Barrier, N., Bianchi, D., Bopp, L.,
744 Bryndum-Buchholz, A., Britten, G. L., Büchner, M., Cheung, W. W. L., Christensen, V., Coll, M.,
745 Dunne, J. P., Eddy, T. D., Everett, J. D., Fernandes-Salvador, J. A., Fulton, E. A., Galbraith, E. D.,
746 Gascuel, D., Guiet, J., John, J. G., Link, J. S., Lotze, H. K., Maury, O., Ortega-Cisneros, K., Palacios-
747 Abrantes, J., Petrik, C. M., du Pontavice, H., Rault, J., Richardson, A. J., Shannon, L., Shin, Y.-J.,
748 Steenbeek, J., Stock, C. A., and Blanchard, J. L.: Next-generation ensemble projections reveal
749 higher climate risks for marine ecosystems, *Nat Clim Change*, 11, 973-981,
750 <https://doi.org/10.1038/s41558-021-01173-9>, 2021.

751 Trinanes, J. and Martinez-Urtaza, J.: Future scenarios of risk of *Vibrio* infections in a warming planet:
752 a global mapping study, *The Lancet Planetary Health*, 5, e426-e435,
753 [https://doi.org/10.1016/S2542-5196\(21\)00169-8](https://doi.org/10.1016/S2542-5196(21)00169-8), 2021.

754 Verfaillie, D., Déqué, M., Morin, S., and Lafaysse, M.: The method ADAMONT v1.0 for statistical
755 adjustment of climate projections applicable to energy balance land surface models, *Geosci.*
756 *Model Dev.*, 10, 4257-4283, <https://doi.org/10.5194/gmd-10-4257-2017>, 2017.

757 Vormoor, K. and Skaugen, T.: Temporal Disaggregation of Daily Temperature and Precipitation Grid
758 Data for Norway, *Journal of Hydrometeorology*, 14, 989-999, [https://doi.org/10.1175/jhm-d-12-](https://doi.org/10.1175/jhm-d-12-0139.1)
759 [0139.1](https://doi.org/10.1175/jhm-d-12-0139.1), 2013.

760 Wang, K. and Clow, G. D.: The Diurnal Temperature Range in CMIP6 Models: Climatology, Variability,
761 and Evolution, *Journal of Climate*, 33, 8261-8279, <https://doi.org/10.1175/jcli-d-19-0897.1>, 2020.

762 Warszawski, L., Frieler, K., Huber, V., Piontek, F., Serdeczny, O., and Schewe, J.: The Inter-Sectoral
763 Impact Model Intercomparison Project (ISI-MIP): Project framework, *Proceedings of the National*
764 *Academy of Sciences*, 111, 3228-3232, <https://doi.org/10.1073/pnas.1312330110>, 2014.

765 [Watters, D., Battaglia, A., and Allan, R.: The Diurnal Cycle of Precipitation according to Multiple](#)
766 [Decades of Global Satellite Observations, Three CMIP6 Models, and the ECMWF Reanalysis,](#)
767 [Journal of Climate, 34, 5063-5080, <https://doi.org/10.1175/JCLI-D-20-0966.1>, 2021.](#)

768 Wehner, M., Lee, J., Risser, M., Ullrich, P., Gleckler, P., and Collins, W. D.: Evaluation of extreme sub-
769 daily precipitation in high-resolution global climate model simulations, *Philosophical Transactions*
770 *of the Royal Society A: Mathematical, Physical and Engineering Sciences*, 379, 20190545,
771 <https://doi.org/10.1098/rsta.2019.0545>, 2021.

Formatiert: Absatz-Standardschriftart

Formatiert: pagelast

Formatiert: Absatz-Standardschriftart

772 Zabel, F. and Mauser, W.: 2-way coupling the hydrological land surface model PROMET with the
773 regional climate model MMS, *Hydrology and Earth System Sciences*, 17, 1705–1714,
774 <https://doi.org/10.5194/hess-17-1705-2013>, 2013.

775 Zabel, F., Mauser, W., Marke, T., Pfeiffer, A., Zängl, G., and Wastl, C.: Inter-comparison of two land-
776 surface models applied at different scales and their feedbacks while coupled with a regional
777 climate model, *Hydrology and Earth System Sciences*, 16, 1017–1031,
778 <https://doi.org/10.5194/hess-16-1017-2012>, 2012.

779 Zabel, F., Müller, C., Elliott, J., Minoli, S., Jägermeyr, J., Schneider, J. M., Franke, J. A., Moyer, E., Dury,
780 M., Francois, L., Folberth, C., Liu, W., Pugh, T. A. M., Olin, S., Rabin, S. S., Mauser, W., Hank, T.,
781 Ruane, A. C., and Asseng, S.: Large potential for crop production adaptation depends on available
782 future varieties, *Global Change Biol*, 27, 3870-3882 <https://doi.org/10.1111/gcb.15649>, 2021.

783 Zhao, W., Kinouchi, T., and Nguyen, H. Q.: A framework for projecting future intensity-duration-
784 frequency (IDF) curves based on CORDEX Southeast Asia multi-model simulations: An application
785 for two cities in Southern Vietnam, *Journal of Hydrology*, 598, 126461,
786 <https://doi.org/10.1016/j.jhydrol.2021.126461>, 2021.